Electronic Supplementary Information

Sulfate Promotion of Selective Catalytic Reduction of Nitric Oxide by Ammonia on Ceria

Linxiao Chen, Vaibhav Agrawal,[†] and Steven L. Tait*

Dept. of Chemistry, Indiana University, Bloomington, Indiana 47405, U. S. A.

* E-mail: tait@indiana.edu, Tel.: +1-812-855-1302

[†] Present address: Indian Institute of Technology, Roorkee, India

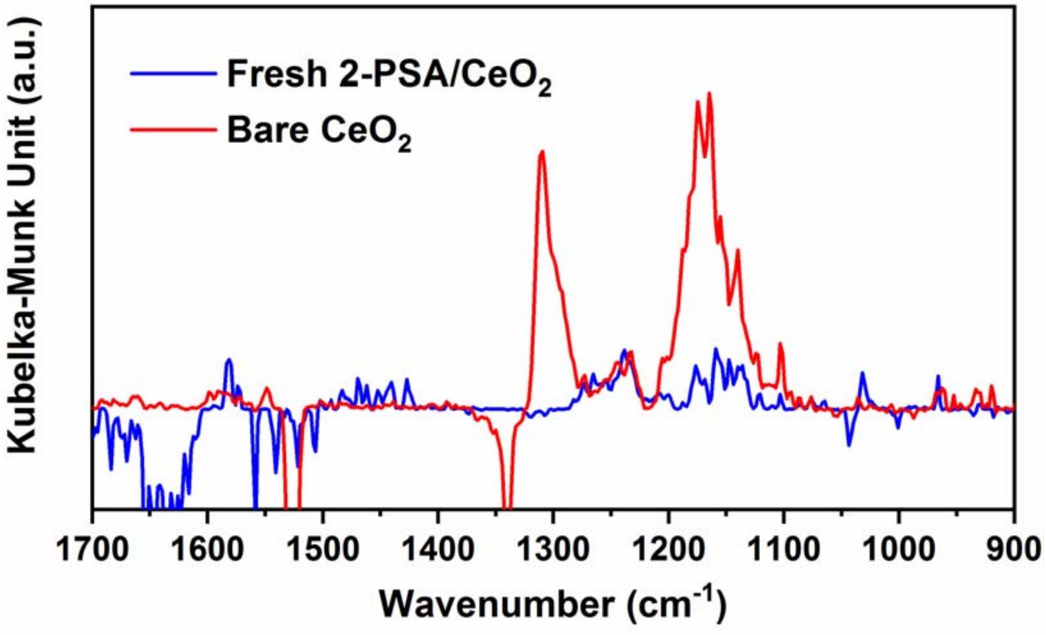

Figure S1. DRIFT spectra of room temperature NH_3 adsorption on fresh 2-PSA/CeO_2 (before O_2 activation) and bare CeO_2. The absence of any NH_3 adsorption peaks ($*NH_3$ or $*NH_4^+$) suggests that the Lewis acid sites from CeO_2 and Brønsted acid sites from 2-PSA are consumed.

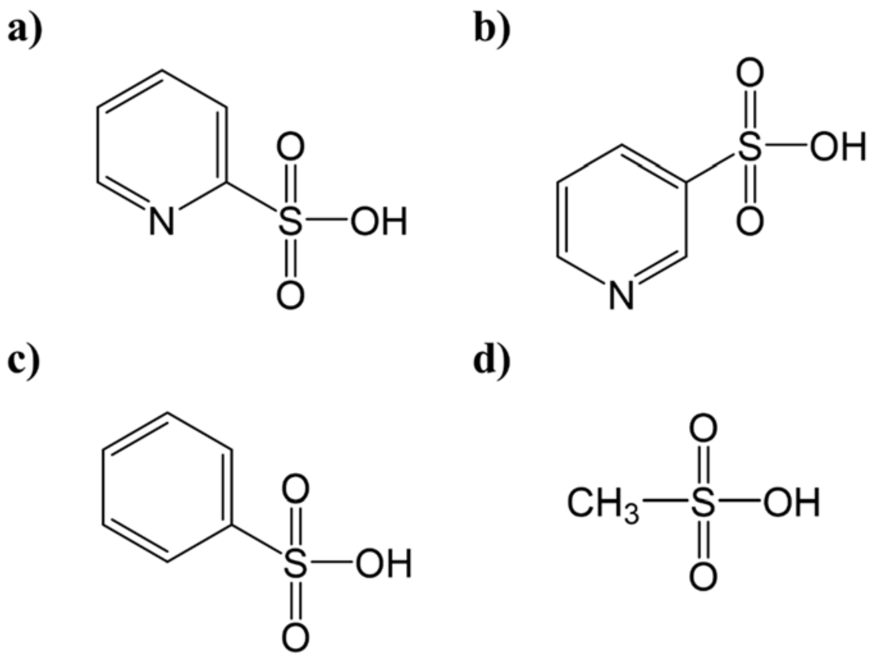

Figure S2. Structure of four organic S precursors used in this work: **(a)** 2-pyridinesulfonic acid (2-PSA), **(b)** 3-pyridinesulfonic acid (3-PSA), **(c)** benzenesulfonic acid (BSA), and **(d)** methanesulfonic acid (MSA).

Table S1. XPS characterizations of sulfated CeO_2 from other S precursors.

Catalyst	N : Ce	S : Ce	N 1*s* BE (eV)	S 2*p* BE (eV)
3-PSA/CeO_2	0.016	0.016	399.6	168.4
BSA/CeO_2	N/A	0.024	N/A	168.9
MSA/CeO_2	N/A	0.036	N/A	168.9

Table S2. Summary of adsorbed species and their corresponding IR features.

Species	Corresponding IR features	Notes
Carbonates (*CO_3)	1200 – 1700 cm^{-1}	
*CO	Around 2000 cm^{-1}	On sulfate-derived Lewis acid sites
*NH_3	1168 cm^{-1}, 1315 cm^{-1} (symm. bending) 1602 cm^{-1} (asymmetric bending) 3300 – 3600 cm^{-1} (stretching) 1355 cm^{-1} (negative)	Specific positions vary on different surfaces; the origin of the 1355 cm^{-1} negative feature is unclear
*NH_4^+	1460 cm^{-1}	Not present on all studied catalysts
*NH_2	1550 cm^{-1}	
*NO	1800 – 2000 cm^{-1}	Not present on all studied catalysts
Nitrates (*NO_3)	1596 cm^{-1} (bridging v_3') 1562 cm^{-1} (bidentate v_3') 1537 cm^{-1} (monodentate v_3') 1170 – 1300 cm^{-1} (v_3'')	The v_3'' peak also splits based on binding configurations, but cannot be distinguished from each other
*NO_2	1616 cm^{-1}	
Bidentate nitro (*O−N−O*)	1373 cm^{-1}	
Nitrosyl (*NO^-)	1010 cm^{-1}	
*NH_2NO_2	1535 cm^{-1} 1253 cm^{-1} 1120 cm^{-1}	Intermediate from the L-H mechanism

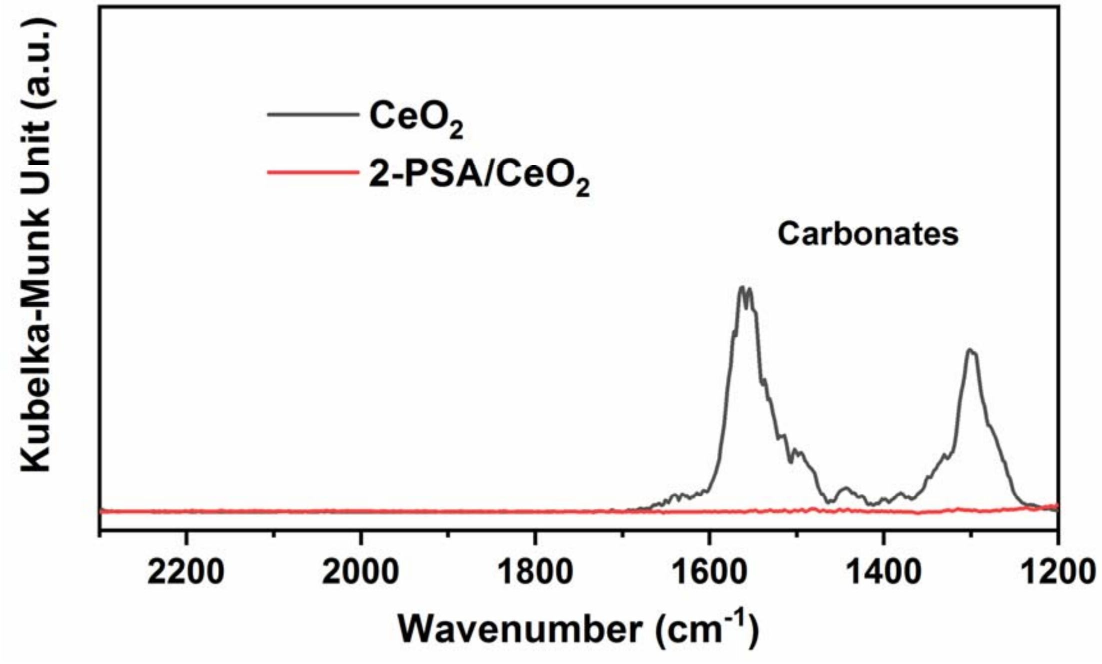

Figure S3. CO adsorption DRIFTS of bare CeO_2 (black) and activated 2-PSA/CeO_2 (red) after Ar purging. Carbonate peaks on CeO_2 are irreversible, and the CO_{ads} peak on 2-PSA/CeO_2 from new Lewis acid sites is reversible.

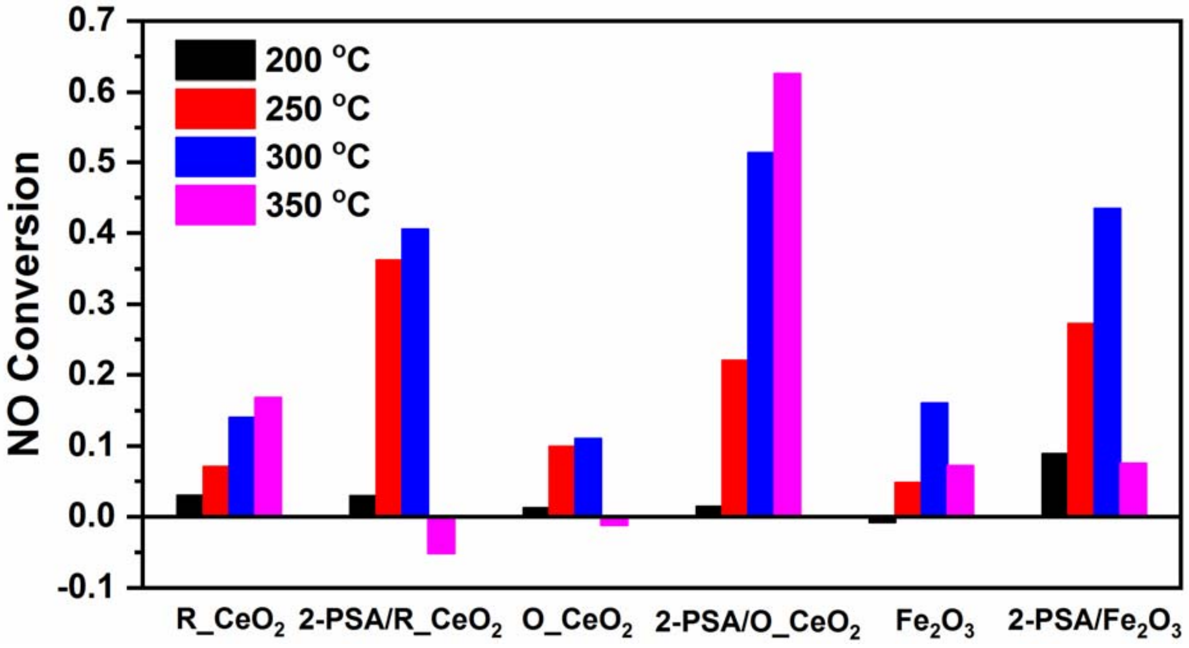

Figure S4. NH_3-SCR activities of reduced CeO_2 (R_CeO_2), oxidized CeO_2 (O_CeO_2), and Fe_2O_3 before and after sulfate deposition, showing the sulfate promotion effect on different surfaces. Apparent negative NO conversions under some conditions are due to NO generated from NH_3 oxidation. Sulfates were deposited with 2-PSA, then O_2 activation was performed.

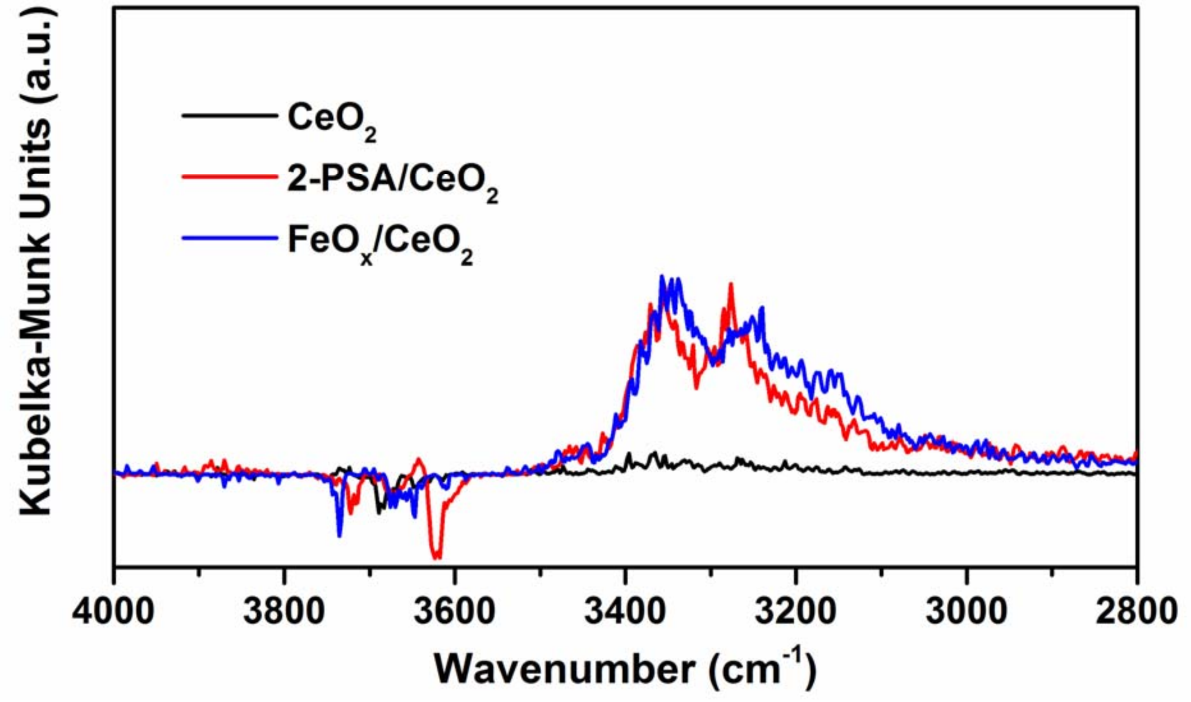

Figure S5. DRIFT spectra of NH_3 adsorption on CeO_2 (black), 2-PSA/CeO_2 (red), and FeO_x/CeO_2 (blue) at 250 °C under 1000 ppm NH_3 in Ar at near-ambient pressure.

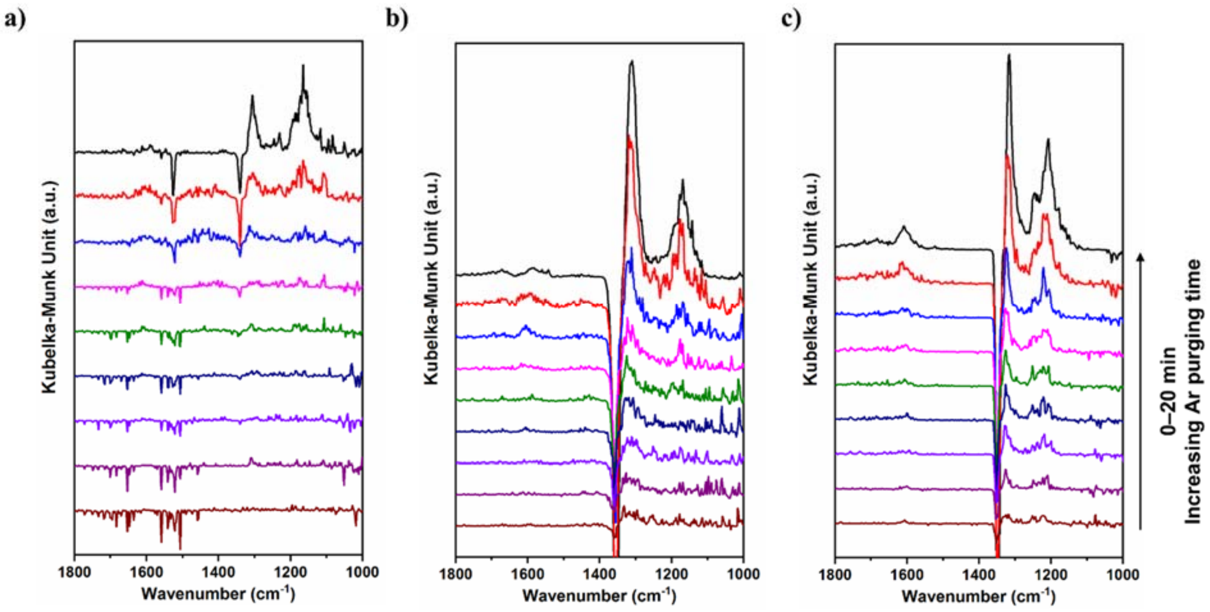

Figure S6. DRIFT spectra with Ar purging time immediately following 30 min NH_3 exposure at 250 °C to observe $*NH_3$ desorption from **(a)** CeO_2, **(b)** 2-PSA/CeO_2, and **(c)** FeO_x/CeO_2. From bottom to top: spectra were collected after 0, 1, 3, 5, 7, 9, 11, 15, and 20 min Ar purging. Peak area was integrated from 1120-1340 cm^{-1} for each spectrum to calculate the relative concentrations in **Figure 5b**.

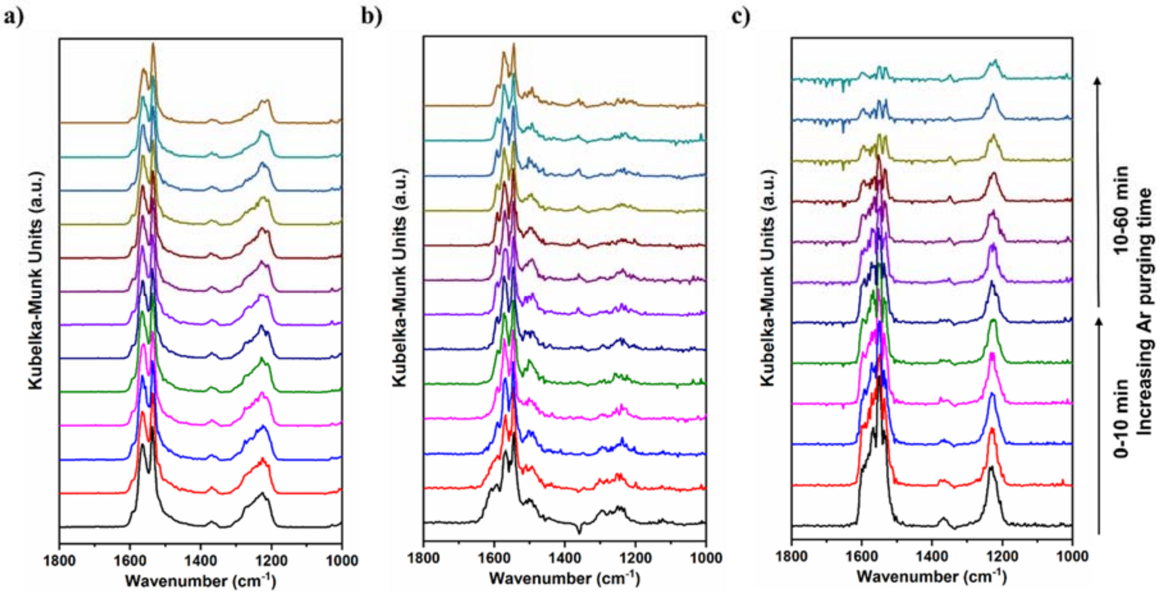

Figure S7. DRIFTS spectra with increasing Ar purging time following NO + O_2 exposure to observe $*NO_3/*NO_2$ desorption from **(a)** CeO_2, **(b)** 2-PSA/CeO_2, and **(c)** FeO_x/CeO_2. From bottom to top, spectra were collected after 0, 1, 3, 5, 7, 9, 11, 15, 20, 30, 40, 50, and 60 min Ar purging. Peak area from 1400-1700 cm^{-1} was integrated to calculate the relative concentrations presented in **Figure 6b**.

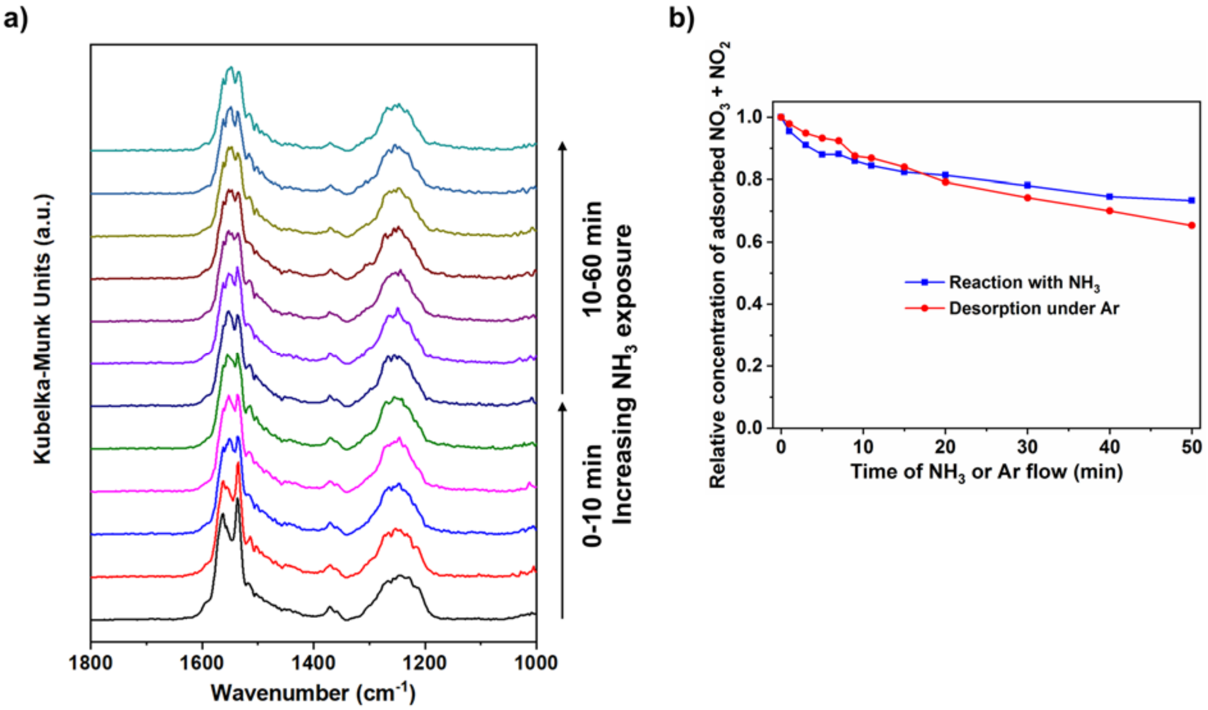

Figure S8. NO-first transient experiment on bare CeO$_2$. **(a)** DRIFTS spectra collected with NH$_3$ exposure time; from bottom to top, spectra were collected after 0, 1, 3, 5, 7, 9, 11, 15, 20, 30, 40, 50, and 60 min NH$_3$ exposure. **(b)** Comparison of the concentration (relative to initial concentration) of *NO$_3$ and *NO$_2$ remaining on bare CeO$_2$ surface when reacting with NH$_3$ (blue) and desorbing under Ar (red), calculated by integrating the region 1400-1700 cm^{-1} in **(a)** and **Figure S7a**, respectively.

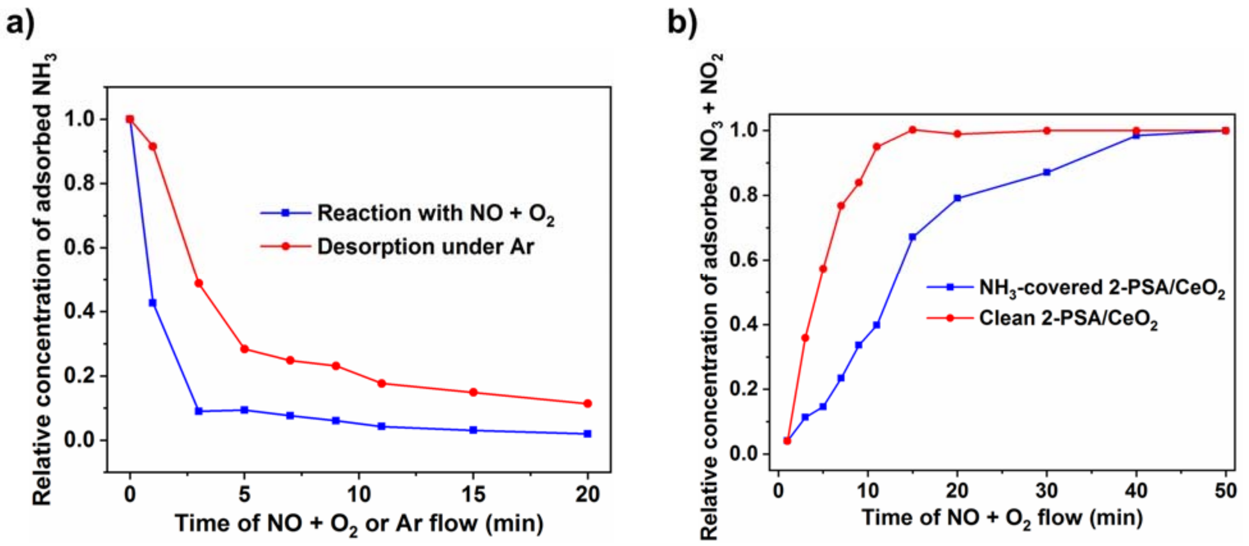

Figure S9. NH_3-first transient experiment on 2-PSA/CeO_2. **(a)** Comparison of the concentration (relative to initial concentration) of *NH_3 on the 2-PSA/CeO_2 surface for reaction with NO + O_2 (blue) or desorption under Ar (red), calculated by integration from 1120-1340 cm^{-1} of the spectra in **Figure 9a** and **S6b**, respectively. NH_3 desorbs faster when reacting with NO + O_2 than when desorbing under Ar. **(b)** Comparison of concentration (relative to saturation concentration) of *NO_3 and *NO_2 on NH3-covered 2-PSA/CeO2 (blue) and on clean 2-PSA/CeO_2 (red), calculated by integration from 1400-1700 cm^{-1} of **Figure 9a** and **S12a**, respectively. NO-derived adsorbates are formed more slowly on the *NH_3-covered surface (blue) than on the clean 2-PSA/CeO_2 surface (red).

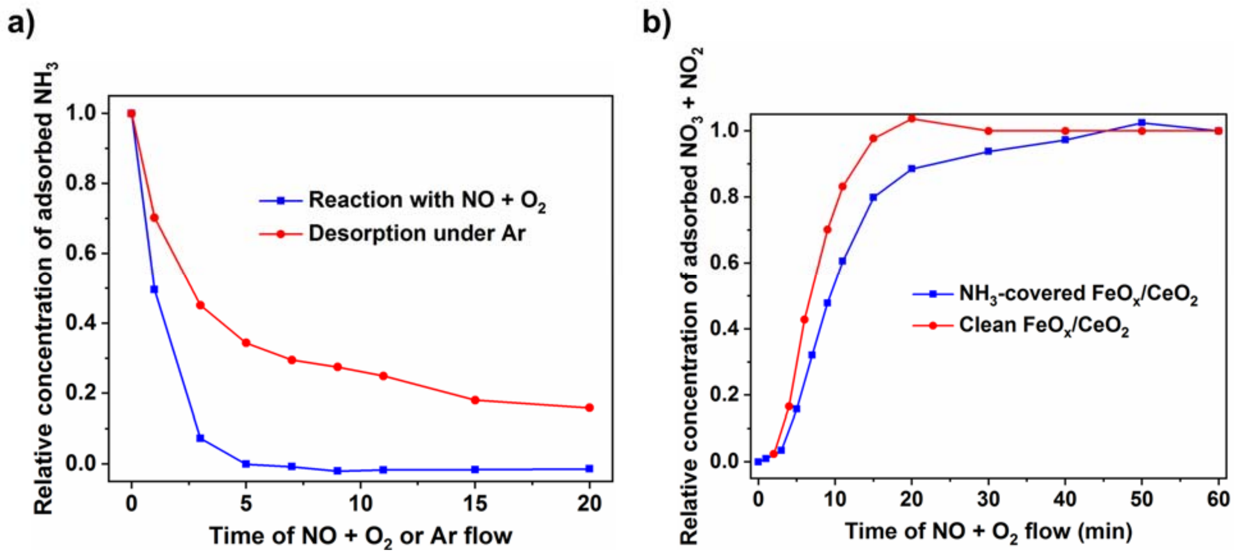

Figure S10. NH_3-first transient experiment on FeO_x/CeO_2. **(a)** Concentration (relative to initial concentration) of $^*NH_3$ on FeO_x/CeO_2 surface showing it desorbs faster when reacting with NO + O_2 (blue) than simply desorbing under Ar (red). Concentrations calculated from integrated area 1120-1340 cm^{-1} of **Figure 9b** and **S6c**, respectively. **(b)** Concentration (relative to saturation concentration) of $^*NO_3$ and $^*NO_2$ on FeO_x/CeO_2 surface. NO-derived adsorbates are formed more slowly on the $^*NH_3$-covered surface (blue) than on the clean FeO_x /CeO_2 surface (red). Concentrations calculated by integration from 1400-1700 cm^{-1} of **Figure 9b** and **S12b**, respectively.

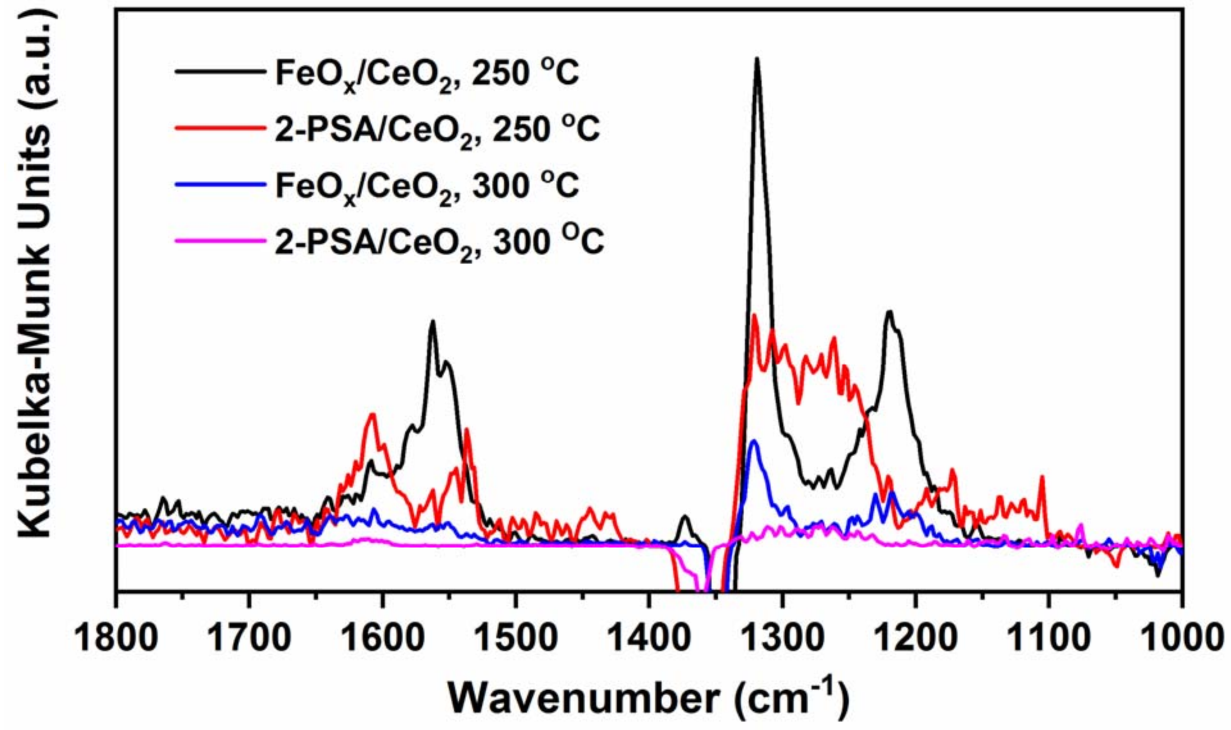

Figure S11. DRIFT spectra collected under actual NH_3-SCR reaction conditions (500 ppm NH_3, 500 ppm NO, 8% O_2, balanced by Ar and N_2) at 250 °C and 300 °C, showing surface adsorbates at steady-state conditions.

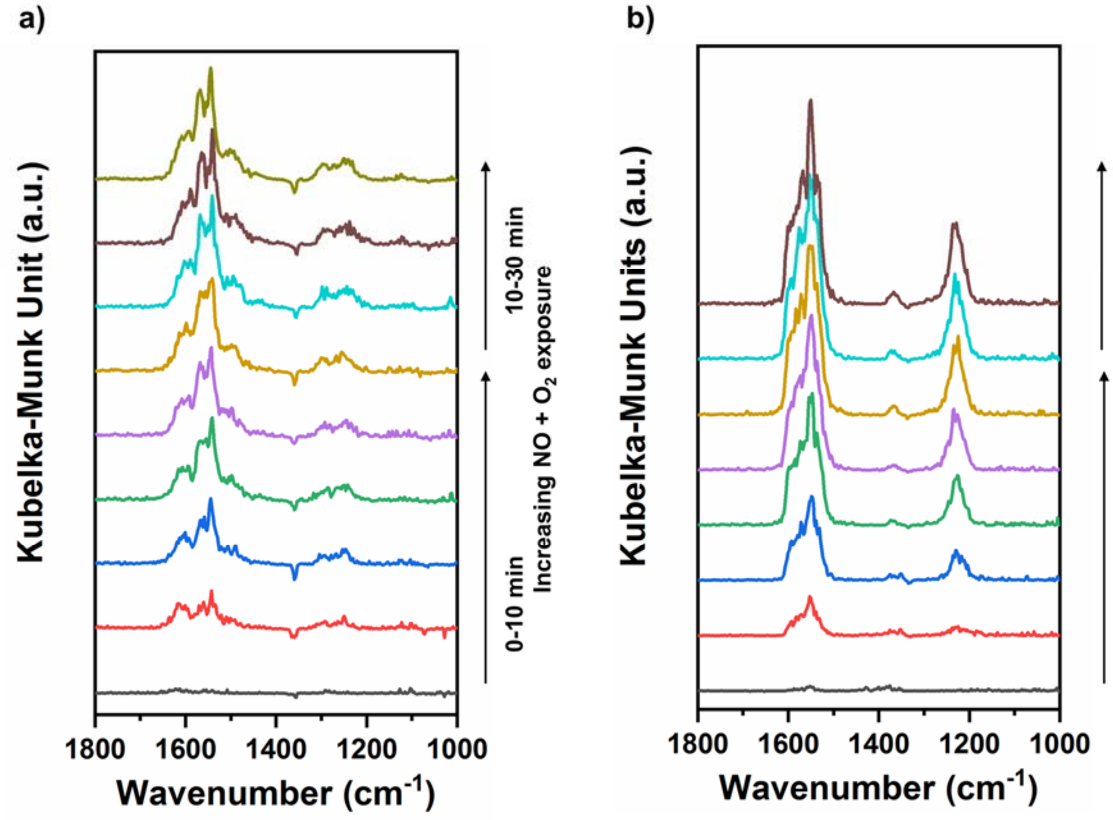

Figure S12. DRIFT spectra with increasing NO + O_2 exposure time to observe *NO_3 and *NO_2 adsorption on **(a)** 2-PSA/CeO_2 and **(b)** FeO_x/CeO_2. From bottom to top, spectra were collected after 0, 2, 4, 6, 8, 10, 15, 20, 25, and 30 min NO + O_2 exposure. Peak area from 1400-1700 cm^{-1} was integrated to calculate the relative concentrations presented in **Figures S9b** and **S10b**.

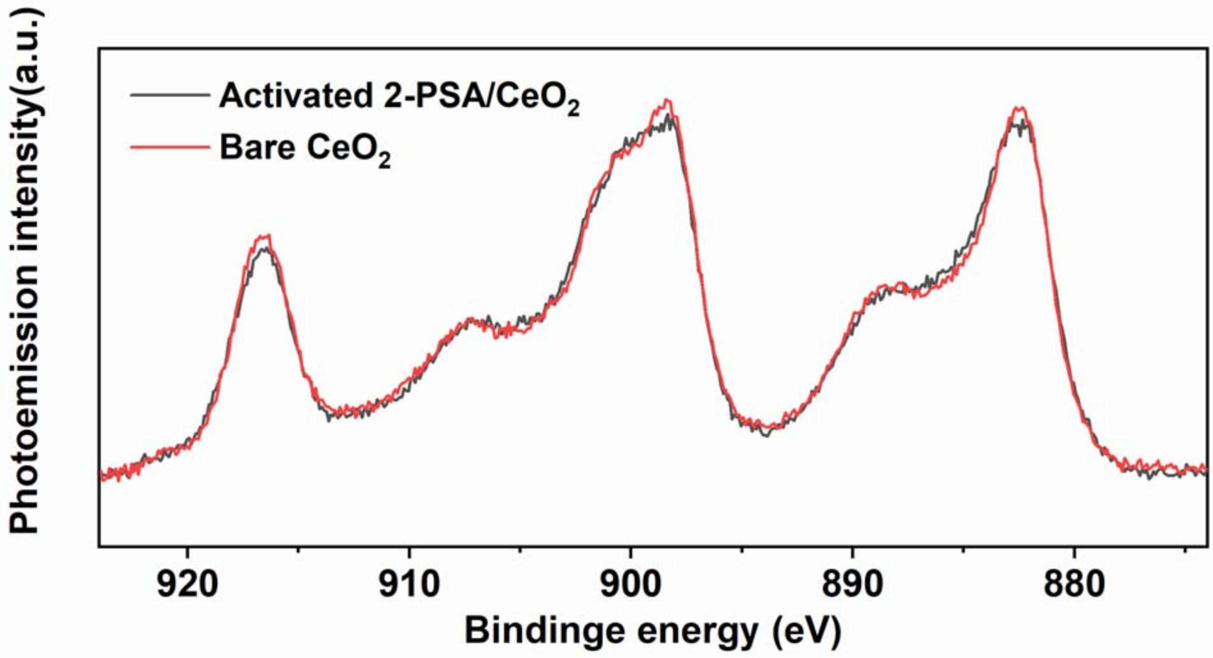

Figure S13. Comparison of Ce 3*d* XP spectra of bare CeO_2 and activated 2-PSA/CeO_2. There is no significant difference between these spectra. Although there is likely to be some change in the Ce^{3+}/Ce^{4+} ratio at the surface, this was not detectable in this measurement, likely due to the large background signal from multiple layers of CeO_2.

Pretreatment conditions

Pretreatment of FeO_x/CeO_2 was made using 10% O_2 at 400 °C for 30 min. This is the standard procedure we have been implementing for the purpose of cleaning surfaces. We used slightly different conditions for 2-PSA/CeO_2, 8% O_2 at 350 °C for 30 min, because that is the highest temperature and O_2 concentration it experiences during the SCR experiments. Initially the reaction was performed without this step, and after 30 min at 350 °C, 2-PSA/CeO_2 catalyst reached full activity, which justifies the choice of this condition. The slight difference between these conditions may have some small impact on surface oxygen species, however, these will be much more significantly impacted by the difference in surface oxygen species due to impregnation of FeO_x or 2-PSA. Changes in surface oxygen after promoter impregnation highlights an advantage of sulfate over FeO_x: it partially deactivates surface-active oxygen while FeO_x does not.